MOLECULAR AND CELLULAR BIOLOGY
2023, VOL. 43, NO. 6, 283–299
https://doi.org/10.1080/10985549.2023.2210033

Taylor & Francis
Taylor & Francis Group

RESEARCH ARTICLE

Dematin Regulates Calcium Mobilization, Thrombosis, and Early Akt Activation in Platelets

Daniel I. Fritz,[a] Yiwen Ding,[b] Glenn Merrill-Skoloff,[c] Robert Flaumenhaft,[c] Toshihiko Hanada,[d] Athar H. Chishti[d]

[a]Programs in Cellular, Molecular and Developmental Biology, Graduate School of Biomedical Sciences, Tufts University School of Medicine, Boston, Massachusetts, USA
[b]Pharmacology and Drug Development, Graduate School of Biomedical Sciences, Tufts University School of Medicine, Boston, Massachusetts, USA
[c]Division of Hemostasis and Thrombosis, Department of Medicine, Beth Israel Deaconess Medical Center, Harvard Medical School, Boston, Massachusetts, USA
[d]Department of Developmental, Molecular, and Chemical Biology, Tufts University School of Medicine, Boston, Massachusetts, USA

ABSTRACT The complex intrinsic and extrinsic pathways contributing to platelet activation profoundly impact hemostasis and thrombosis. Detailed cellular mechanisms that regulate calcium mobilization, Akt activation, and integrin signaling in platelets remain incompletely understood. Dematin is a broadly expressed actin binding and bundling cytoskeletal adaptor protein regulated by phosphorylation via cAMP-dependent protein kinase. Here, we report the development of a conditional mouse model specifically lacking dematin in platelets. Using the new mouse model termed PDKO, we provide direct evidence that dematin is a major regulator of calcium mobilization, and its genetic deletion inhibits the early phase of Akt activation in response to collagen and thrombin agonists in platelets. The aberrant platelet shape change, clot retraction, and in vivo thrombosis observed in PDKO mice will enable future characterization of dematin-mediated integrin activation mechanisms in thrombogenic as well as nonvascular pathologies.

KEYWORDS platelets, calcium signaling

INTRODUCTION

Dematin is an F-actin-binding cytoskeletal adaptor protein essential for maintaining erythrocyte (RBC) shape and membrane stability.[1,2] Its modular structure of ~50 kDa consists of a C-terminal headpiece domain shared with the villin family of cytoskeletal proteins.[3–5] The large N-terminal core domain of dematin is somewhat unique, showing sequence similarity to its closest homolog abLIM (Fig. 1A)[4,6] but not with other members of the villin family. Dematin's broad expression in most tissues along with its regulation by phosphorylation by multiple protein kinases merits its functional evaluation in nonerythroid cells.[7–9,10] Furthermore, the location of the dematin gene (*DMTN* or *EBP49*) on human chromosome 8p21.3,[11] a region frequently mutated in tumors including B-cell lymphomas,[12] is notable and increases the putative translational applications of further investigation of dematin function.

Using immune-electron microscopy, our previous studies visualized dematin as well as adducin at the spectrin-actin junctions, which are critical for the regulation of RBC membrane mechanical properties.[13] A similar spectrin-based network attaches and supports the plasma membrane in anucleate platelets.[14] Unlike mature RBCs, platelets serve as a relatively tractable cell system to evaluate cell shape as well as multiple signaling pathways elicited by a variety of agonists.[15–19] Since dematin is abundant both in human and mouse platelets,[19,20] we have utilized mouse gene deletion approaches to interrogate dematin's function in platelets. Originally, we developed a mouse model with the systemic deletion of the headpiece domain of dematin.[19] The headpiece knockout (HPKO) mice expressing the core domain of dematin showed a mild

Address correspondence to Athar H. Chishti, athar.chishti@tufts.edu.

The authors declare no competing financial interests.

Received 22 March 2023
Revised 19 April 2023
Accepted 21 April 2023

phenotype of RBC shape change and hemolysis.[19] The relatively mild anemia in HPKO mice[1] enabled us to evaluate the functional role of dematin's headpiece domain in platelets. Our previous studies demonstrated that dematin lacking its headpiece domain is unable to regulate calcium mobilization in platelets.[19] While these studies were informative, a valid issue was raised about the functional role of the core domain of dematin that was stably expressed in the HPKO platelets.[19] To address this concern, we generated a conditional mouse knockout (KO) of the full length of dematin (FLKO).[2] Remarkably, the systemic deletion of full-length dematin resulted in nearly complete fragmentation of RBCs, acute hemolysis, and unsustainable anemia in the long-term.[2] While these studies demonstrated an essential role of the core domain in maintaining dematin function in RBCs, the FLKO model was not suitable to study platelet functions due to massive hemolysis in vivo.[2]

Here, we report the generation and characterization of the first tissue-specific deletion of the dematin gene in platelets. Using a multi-stage Cre-LoxP gene deletion strategy, we generated a platelet-specific dematin knockout model termed PDKO by employing a megakaryocyte-specific platelet factor 4 (Pf4) promoter-driven genetic recombination of the *DMTN* gene. This genetic approach enabled us to perform platelet function analysis without the deletion of dematin in other cell types, including RBCs. Our results demonstrate a functional role of dematin in platelet shape change, calcium mobilization, integrin signaling, and in vivo thrombosis. Importantly, dematin emerges as a positive regulator of early Akt activation in platelets with implications in signaling and actin cytoskeletal reorganization in other cell types.

RESULTS

Generation and validation of platelet dematin null mouse model (PDKO). Previously, our laboratory generated the FLKO mouse model using a targeted gene insert in the *DMTN* (*EBP49*) gene to induce a null allele.[2] This mouse model contained FRT and LoxP sites for flippase and Cre recombination. Breeding of this mouse line with a flippase-expressing line generated an allele with integrated loxP sites flanking exons 5 and 8 (Fig. 1B, top). The allele was transcriptionally intact thus retaining normal

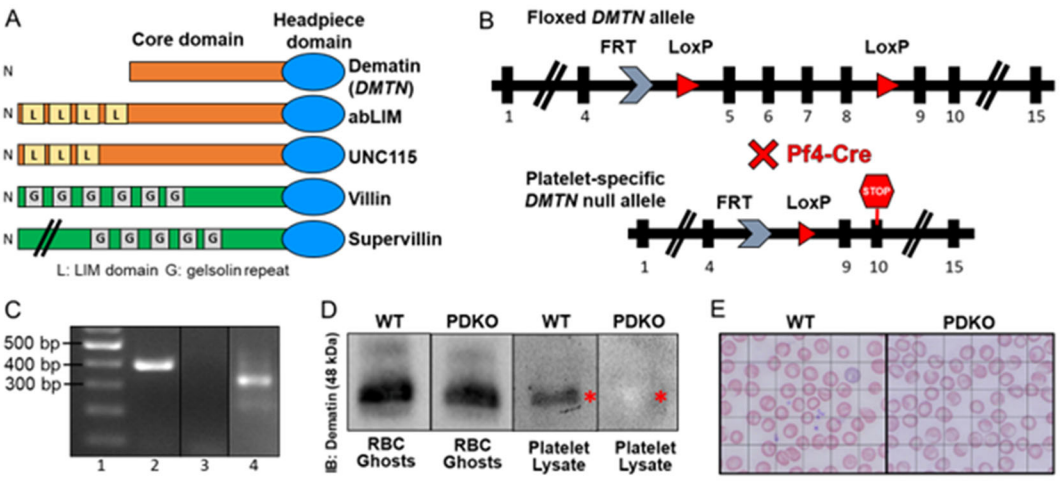

FIG 1 Generation of the PDKO mouse model. (A) Dematin is homologous to the villin-family of proteins. Dematin shares its headpiece domain with villin and supervillin, but its core domain is characteristically distinct. Unique gelsolin repeats are labeled as "G" in villin and supervillin. Dematin shares its core domain with abLIM and UNC115 but lacks the LIM domains labeled as "L." (B) Mice homozygous for the *DMTN* (dematin) floxed allele containing loxP sites are crossed with Pf4-Cre expressing mice to recombine exons 5 through 8 of the *DMTN* gene. This yields a frame shift creating a premature stop codon in exon 10 generating an unstable dematin transcript that degrades and is not translated. (C) Genotyping strategy for PDKO mice. Pf4-Cre genotyping was performed using the Pf4-Cre forward primer: *CCA AGT CCT ACT GTT TCT CAC TC* and the Pf4-Cre reverse primer *TGC ACA GTC AGC AGG TT* resulting in an expected 400 bp amplicon. *DMTN* floxed/floxed genotyping was tested using *DMTN* floxed/floxed forward primer: *GCC GGC TGA CTT AAG TGG GAT CC* and *DMTN* floxed/floxed reverse primer: *GTT TTC CAG GGT GAC AGC TGT TCA* resulting in an expected 351 bp amplicon. Lane 1: DNA marker, Lane 2: PDKO mouse Pf4-Cre genotyping, Lane 3: WT mouse Pf4-Cre genotyping, Lane 4: *DMTN* floxed/floxed genotyping. (D) Dematin protein expression in WT and PDKO RBCs and platelets. The expected 48 kDa size band is marked by a red asterisk in platelet samples. (E) Wright stain of WT and PDKO blood smears.

expression of dematin protein. A series of crosses with platelet factor 4-Cre mice (Pf4-Cre) resulted in the generation of mice with the following genotypes: Pf4-Cre +/–; *DMTN* f/f mice and Pf4-Cre –/–; *DMTN* f/f (Fig. 1B). The Cre recombination of exons 5–8 yielded a frame shift and a premature stop codon in exon 10, preventing translation of dematin protein (Fig. 1B, bottom). The use of the Pf4 promoter restricted Cre expression to the megakaryocyte lineage. Mice lacking dematin in platelets were designated as "platelet dematin knockout" (PDKO) and mice not expressing Pf4-Cre were designated "WT." Mice were genotyped for Pf4-Cre (400 base pair expected size; Fig. 1C, lanes 2 and 3) and *DMTN* f/f alleles (351 base pair expected band size; Fig. 1C, lane 4). PDKO mice genotyped positive for Pf4-Cre (Fig. 1C, lane 2), while WT mice genotyped negative for Pf4-Cre (Fig. 1C, lane 3). Dematin protein expression was detected in WT and PDKO RBCs, however, dematin expression was not observed in purified, washed PDKO platelets, validating that dematin expression in platelets was lost (Fig. 1D, the asterisk indicates the expected protein size of 48 kDa). As expected, RBC morphology was unaltered in the PDKO mice (Fig. 1E). Together, these data provide experimental evidence for the generation of the platelet-specific dematin null mouse model used in this study.

Hematological analysis of PDKO model. PDKO mice were bred on a C57B/6J genetic background. PDKO mice were born at the expected Mendelian ratio of 1:1, and adult mice appeared healthy with no discernible anomalies. Routine necropsy did not show any discernible changes in the anatomy of major organs of mutant mice (data not shown). Complete blood count (CBC; IDEXX BioAnalytics) of adult PDKO mice under steady-state conditions revealed normal blood cell parameters, including the platelet count and volume (Fig. 2A). For subsequent platelet characterization, it was necessary to evaluate the status of RBCs due to the emerging evidence for physiological interactions between platelets and RBCs.[21] Wright–Giemsa staining and SDS-PAGE analysis showed no distinct changes in the RBC shape and membrane proteins of PDKO mice (data not shown). No nucleated RBCs and Heinz bodies were detected in the peripheral blood of PDKO mice. Finally, the PDKO mice were examined for any bleeding diathesis. No statistical difference in the tail bleeding time was observed between wild-type (WT) and PDKO mice (Fig. 2B). Unlike our previous dematin headpiece and full-length whole-body knockout mouse models,[1,2] the PDKO mice do not show any hemolysis concerns and therefore serve as a suitable model system for platelet function studies as outlined below.

PDKO mice exhibit broad platelet aggregation defects. Given that the core domain of dematin is critical for maintaining the cell shape and membrane stability,[2,22]

A

Hematology	WT	PDKO	Hematology	WT	PDKO
Platelet count (K/μL)	612.5	545	WBC (K/μL)	9.65	8.3
RBC (M/μL)	6.87	6.95	Lymphocytes (%)	85.05	87.15
MCV (fL)	46.5	47.5	Neutrophils (%)	8.9	7.15
HCT (%)	31.9	32.65	Monocytes (%)	3.6	3.85
HGB (g/dL)	10	10.25	Eosinophils (%)	2.45	1.85
MCHC (g/dL)	31.35	31.35	MPV (fL)	6.9	6.7
Absolute reticulocyte (K/μL)	182	225	MPV (fL)	6.1	6.6
Reticulocyte (%)	2.65	3.2	PDW (fL)	8.1	6.9
MCH (pg)	14.6	14.75	PDW (fL)	7.4	7.8

B

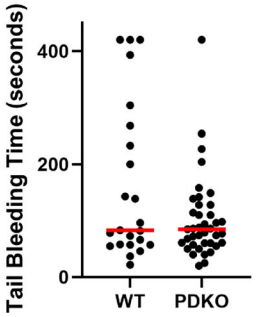

FIG 2 Hematological analysis of PDKO mice. (A) Complete blood count (CBC) of WT and PDKO blood samples. RBC (red blood cells), MCV (mean corpuscular volume), HCT (hematocrit), HGB (hemoglobin), MCHC (mean corpuscular hemoglobin concentration), MCH (mean corpuscular hemoglobin), WBC (white blood cells), MPV (mean platelet volume), PDW (platelet distribution width). (B) Tail bleeding time assay with statistical median: WT 80 s, PDKO 82 s. 25–30 mice of each genotype were used for the tail bleeding measurements. WT: 124.50 ± 102.1; PDKO: 93.76 ± 52.66, *P* value 0.1346.

we hypothesized that the deletion of full-length dematin may lead to functional defects in platelets. To investigate this possibility, we measured the platelet aggregation response of multiple agonists by transmission light aggregometry (Fig. 3). PDKO platelets showed attenuated aggregation response to thrombin (Fig. 3A and B), TRAP4 (thrombin receptor activating peptide 4, a PAR4 specific agonist (Fig. 3C), collagen (Fig. 3D), CRP (collagen related peptide) (Fig. 3E), U46619 (a synthetic agonist of thromboxane A_2) (Fig. 3F), and ADP (Supplemental Fig. 1A). PDKO platelet aggregation tracings by multiple agonists indicated two potential nodes of functional defects. PDKO platelets showed reduced shape change in response to thrombin (Fig. 3A) and collagen (Fig. 3D) as indicated by a brief decrease in light transmission immediately after agonist stimulation. This finding is consistent with the essentiality of dematin's core domain in the regulation of cellular shape in RBCs and fibroblasts.[2,22] Furthermore, the deletion of dematin predominantly impaired the progression of secondary platelet aggregation response by agonists (Fig. 3C; arrow depicts phase 2). These findings suggest that dematin may play a functional role in the regulation of downstream signaling

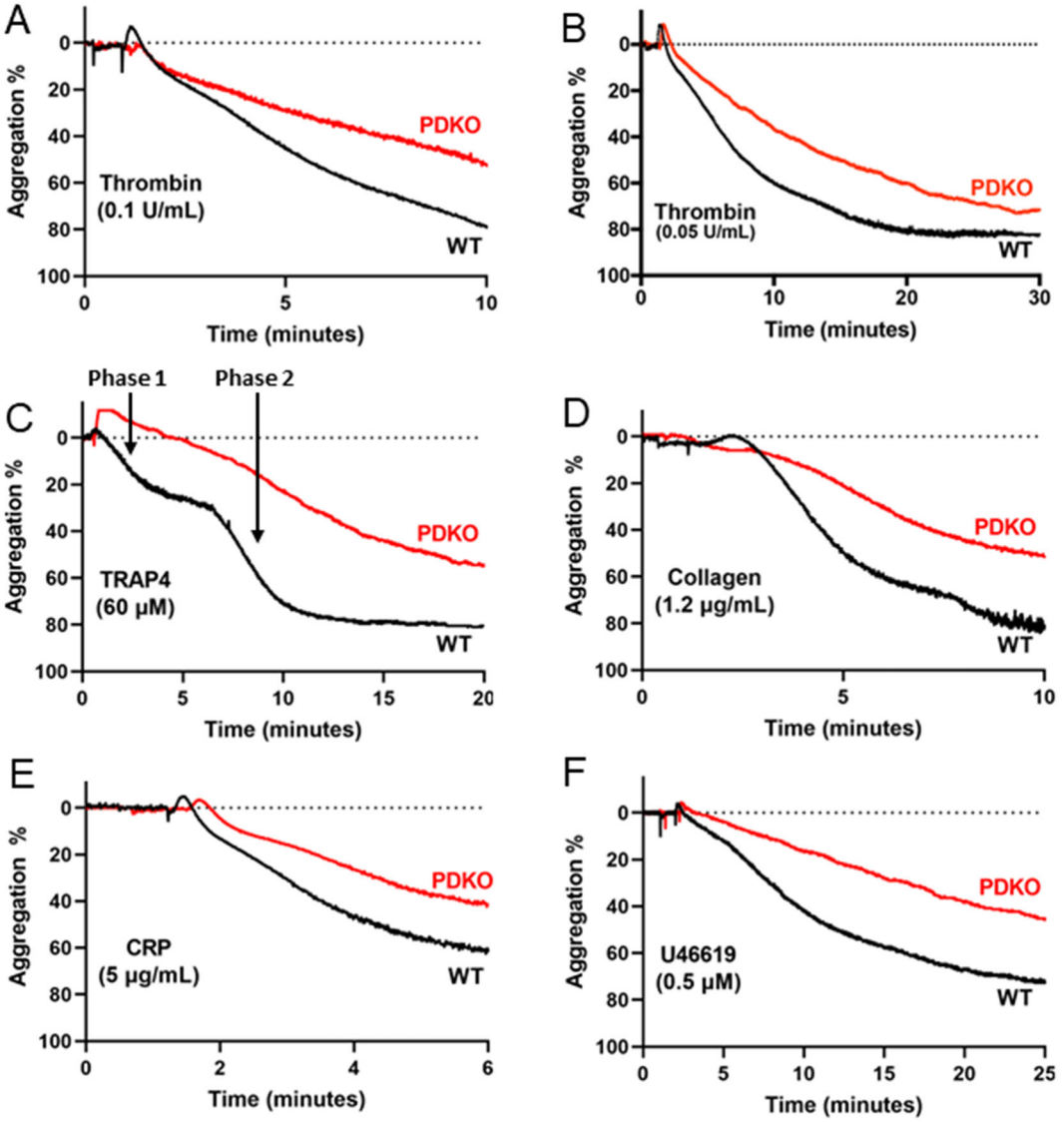

FIG 3 Platelet aggregation responses to agonists in WT and PDKO. Platelet aggregation response to (A) Thrombin (0.1 U/mL), (B) Thrombin (0.05 U/mL), (C) TRAP4 (60 μM), (D) collagen (1.2 μg/mL), (E) CRP (5 μg/mL), and (F) U46619 (0.5 μM). TRAP4-induced activation of WT platelets shows two distinct aggregation phases marked by arrows 1 and 2. TRAP4 (thrombin receptor activating peptide 4, a PAR4 specific agonist). CRP (collagen-related peptide). U46619 (a synthetic agonist of thromboxane A2). Quantification of thrombin-stimulated aggregation is shown in Supplemental Fig. 4B.

pathways common to multiple platelet agonist receptors, which may be impacted by the secretion of platelet granules.

Dematin regulates platelet granule secretion. Platelets utilize positive feedback mechanisms for their activation in an autocrine and paracrine fashion by regulating the secretion of dense granules and α-granules.[23–25] To determine how the deletion of full-length dematin impacts granule secretion, the ATP secretion response of PDKO platelets to multiple agonists was measured. The results revealed broad inhibition of dense granule release in response to thrombin (Fig. 4A; dose-response curves are shown in Supplemental Fig. 1B and C), TRAP4 (Fig. 4B), collagen (Fig. 4C), and U46619 (Fig. 4D). As expected, the U46619 mediated stimulation of WT platelets resulted in a characteristic "two-phase" dense granule secretion process (Fig. 4D). Interestingly, the dense granule secretion response of PDKO platelets by U46619 showed a reduced but essentially intact first phase of the secretion process (Fig. 4D). In contrast, the second phase of the dense granulation was completely ablated in PDKO platelets (Fig. 4D, arrow). These results illustrate a generalized inhibition of dense granule release in PDKO platelets. Next, we evaluated the status of α-granule secretion response in PDKO platelets. The surface expression of P-selectin was measured by flow cytometry. In response to thrombin stimulation, P-selectin expression, a common marker of α-granule release, was significantly reduced in the PDKO platelets (Fig. 4E). The reduced secretion of both dense and α-granules is consistent with broad inhibition of platelet aggregation by multiple agonists observed in PDKO platelets (Fig. 3). Impaired platelet granule secretion defects in PDKO mice suggest that dematin may regulate self-positive feedback loops, thus impacting integrin signaling and downstream clotting cascades.

Dematin loss attenuates platelet integrin signaling and clot retraction. Our findings from PDKO mice indicating the involvement of dematin in shape change suggest a potential functional impact of "inside-out" signaling on platelet integrin (GPIIb/IIIa or αIIb/β3) activation and subsequent downstream "outside-in" signaling pathways resulting in clot retraction and platelet spreading phenotypes. Using the fluorescent-tagged JON/A monoclonal antibody (GPIIb/IIIa, CD41/CD61)-PE), which binds to the high-affinity conformation of integrin, we measured integrin activation upon thrombin

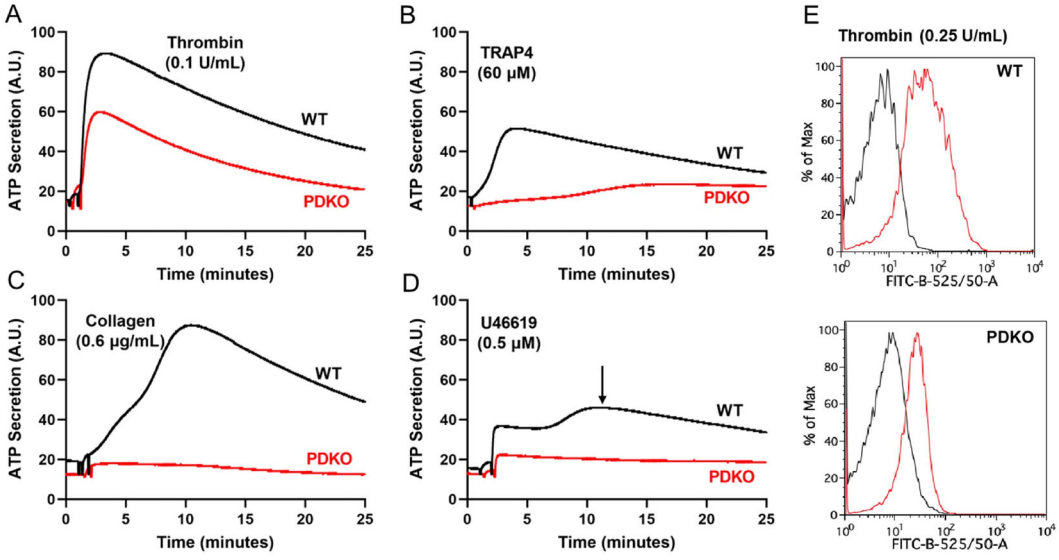

FIG 4 Platelet secretion responses to agonists in WT and PDKO platelets. Platelet dense-granule release responses to agonists: (A) thrombin (0.1 U/mL), (B) TRAP4 (60 μM), (C) collagen (0.6 μg/mL), and (D) U46619 (0.5 μM). The black arrow indicates the peak dense-granule release during the second phase of secretion. Dense-granule release was assessed using the Chrono-Lume reagent. (E) WT (top) and PDKO (bottom) platelet α-granule release in response to thrombin (0.25 U/mL). Unstimulated conditions are represented by the black tracing; stimulated conditions are represented by the red tracing. Stimulation and increased α-degranulation is represented by a rightward shift on the *x*-axis. The measured fold increase of the geometric mean fluorescence intensity from unstimulated to stimulated samples: WT = 8.7, PDKO = 3.17. The α-granule secretion was measured by flow cytometry of P-selectin surface expression.

stimulation of platelets by flow cytometry. The results revealed that integrin activation in PDKO platelets was attenuated at a lower concentration of thrombin (0.0125 U/mL) as reflected by the reduced rightward shift of the antibody mean fluorescence intensity compared to WT (Fig. 5A). A minimal difference in integrin activation was observed at a higher concentration of thrombin (0.25 U/mL) (Fig. 5B). These findings suggest that dematin is required for proper integrin activation as a part of inside-out signaling. To evaluate the integrity of outside-in signaling, the clot retraction phenotype was evaluated in PDKO mice. Upon stimulation by thrombin, clot retraction was impaired in PDKO platelets within 3 h but recovered fully after 20 h (Fig. 5C). Consistent with reduced integrin activation in PDKO platelets, these findings demonstrate that the loss of dematin disrupts inside-out signaling and integrin activation as well as outside-in signaling and clot retraction pathways.

Dematin regulates platelet spreading and lamellipodia formation. To further investigate the impact of outside-in signaling on cell shape regulation, we assessed the capacity of platelet spreading in PDKO platelets. Dematin is an actin-binding and bundling cytoskeletal protein essential for maintaining RBC shape and membrane stability.[3,7,10,13] Notwithstanding its abundant expression in mature erythrocytes and platelets, the precise role of full-length dematin in platelet shape changes and spreading remains incompletely understood. We evaluated the morphological features of platelets from PDKO mice using fluorescence and scanning electron microscopy (SEM). Washed platelets were spread over fibrinogen-coated coverslips and platelet spreading was monitored over 30 min by Phalloidin-staining of actin filaments (Fig. 6A). Significant differences in the spreading of PDKO platelets were observed after incubation on fibrinogen-coated coverslips (Fig. 6A and B). In contrast to WT platelets, the PDKO platelets remained relatively smaller and rounded at both 15- and 30-min time

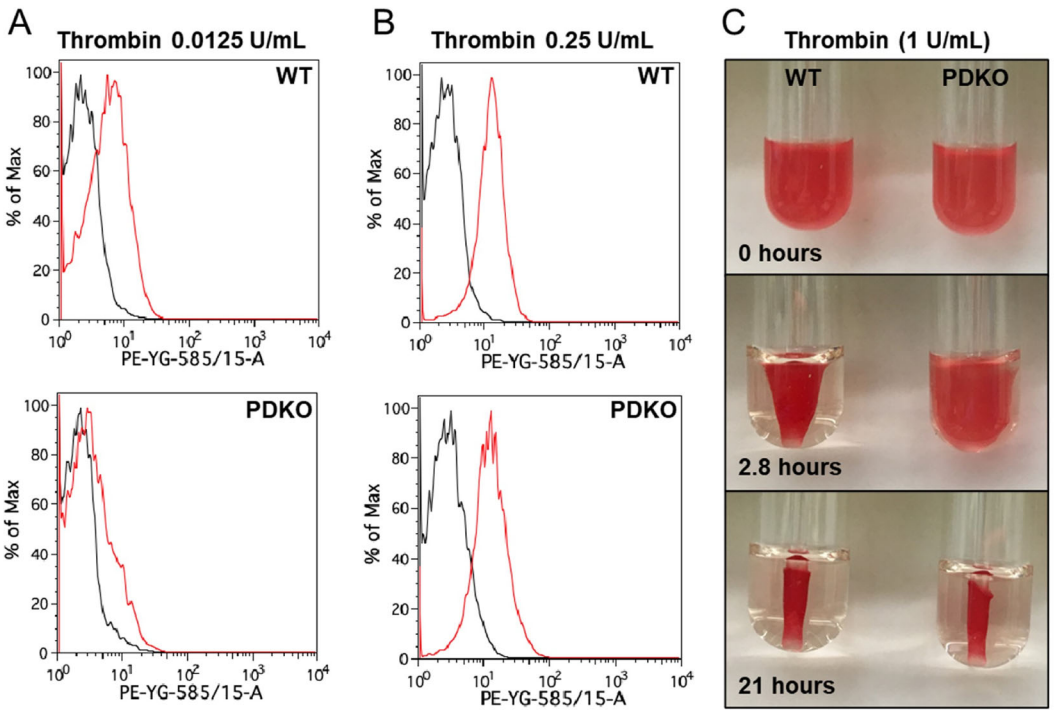

FIG 5 Integrin activation and clot retraction responses in WT and PDKO platelets. (A and B) WT (top) and PDKO (bottom) integrin activation in response to thrombin (A) (0.0125 U/mL) and (B) (0.25 U/mL). Unstimulated conditions are represented by the black tracing; stimulated conditions are represented by the red tracing. Increased integrin activation is represented by a rightward shift on the *x-axis*. The measured fold increases of the geometric mean fluorescence intensity from unstimulated to stimulated samples: (A), WT = 2.20, PDKO = 1.44; (B), WT = 4.65, PDKO = 4.11. Platelets supplemented with 1.0 mM calcium were incubated with thrombin and PE-conjugated antibody against integrin alphaIIbbeta3 (GPIIb/IIIa, CD41/CD61)-PE) for 15 min. Reaction was quenched with PBS, and samples were analyzed by flow cytometry using the established protocols from Emfret Analytics (https://www.emfret.com/index.php?id=6). (C) Clot retraction response over time in WT and PDKO platelet-rich plasma (PRP) stimulated with thrombin (1 U/mL). Quantification of clot retraction is shown in Supplemental Fig. 4A.

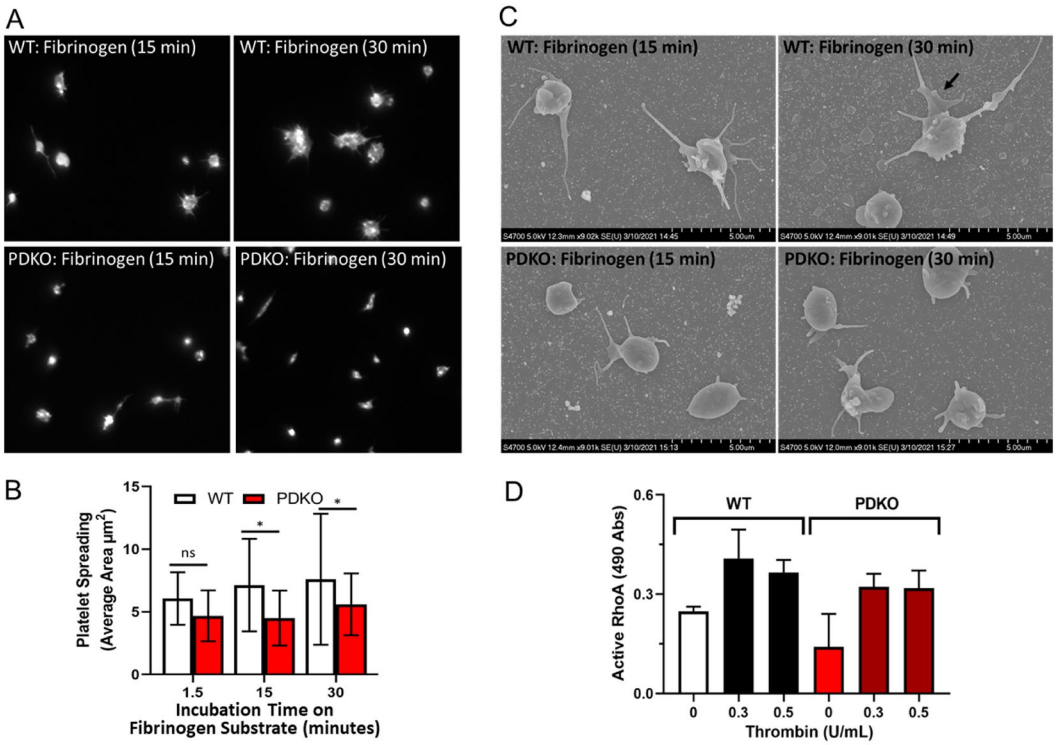

FIG 6 Platelet spreading response and RhoA activation. (A) WT (top) and PDKO (bottom) platelet spreading on fibrinogen-coated surfaces for 15 (left) or 30 (right) min. Fluorescence staining of actin using AF594 phalloidin. Magnification 100×. (B) Average platelet spreading area (μm^2). Mean values: 1.5 min – WT 6.07 μm^2, PDKO 4.68 μm^2; 15 min – WT 7.14 μm^2, PDKO 4.51 μm^2; 30 min – WT 7.6 μm^2, PDKO 5.6 μm^2. n-number: 1.5 min – WT 12, PDKO 15; 15 min – WT 104, PDKO 53; 30 min – WT 189, PDKO 143. ns = not significant, *P value < 0.0001. (C) Scanning electron microscopy of WT (top) and PDKO (bottom) platelet spreading on fibrinogen for 15 (left) and 30 (right) min. The arrow indicates lamellipodia structure in WT platelets. Magnification 9000×. Note: Larger images of Fig. 6A and C are shown in Supplemental Fig. 2A and B. (D) RhoA activation in WT and PDKO platelets in response to thrombin. RhoA activity was measured at 490 nm absorbance. Average absorbance values at 490 nm: Unstimulated – WT (0.2480), PDKO (0.1406), not significant; thrombin 0.3 U/mL: WT (0.4077), PDKO (0.3223), not significant; thrombin 0.5 U/mL: WT (0.3658), PDKO (0.3181), not significant. Statistical analyses were performed by Student's *t*-test.

points with limited attachment and spreading (Fig. 6A). Time-dependent quantification of spreading indicated no significant differences between WT and PDKO platelets at the 1.5-min time point; however, a significant reduction in the average PDKO cell area was observed at both 15- and 30-min compared to WT platelets (Fig. 6B).

To further investigate morphological differences between WT and PDKO platelets, washed platelets were spread over immobilized fibrinogen and visualized by SEM after 15- and 30-min of incubation (Fig. 6C). After incubation for 15 min, the PDKO platelets appeared more rounded showing reduced spreading on fibrinogen substrate relative to WT platelets (Fig. 6C; a higher magnification of this image is shown in Supplemental Fig. 2A). After 30 min of incubation, the PDKO platelets remained rounded and displayed limited attachment, more cellular rounding, and limited filopodial extensions. Notably, PDKO platelets displayed a striking lack of lamellipodia formation compared to WT platelets (Fig. 6C, arrow; higher magnification of this image is shown in Supplemental Fig. 2B). However, this imaging technique does not allow us to rule out the possibility that dematin loss indirectly impacts the spreading and actin filament organization of filopodia in platelets.

Integrin outside-in signaling in platelets is regulated by a complex interplay between tyrosine kinases, including Src, multiple adaptor proteins, RhoA, and the actin cytoskeleton.[15,26] RhoA activation is a key readout of cytoskeleton-mediated signaling in platelets.[15,27,28] We evaluated the status of RhoA in resting and thrombin-stimulated PDKO platelets. RhoA activation was measured in platelets activated for 1 min in the presence of thrombin at 0.3 U/mL and 0.5 U/mL using a commercial ELISA kit (Cytoskeleton Inc.). The observed RhoA activation in WT and PDKO platelets suggested

that the PDKO platelets exhibit elevated RhoA activation in a differential manner (unstimulated to thrombin 0.3 U/mL: WT = 1.64× increase, PDKO = 2.29× increase) (Fig. 6D). However, data from multiple experiments showed batch-to-batch variability in the resting platelets that could contribute to the observed variability in RhoA activation. Therefore, we conclude that the fold increase in RhoA activation is not statistically significant between WT and PDKO platelets under these conditions.

Dematin regulates intraplatelet calcium mobilization. Previously, we have shown a functional role of the headpiece domain of dematin in calcium mobilization using our systemic HPKO mouse model.[19] To evaluate the functional role of the core domain of dematin, we tested calcium mobilization in PDKO platelets. Washed WT and PDKO platelets were supplemented with 2.0 mM calcium and stimulated by thrombin (0.5 U/mL). Calcium mobilization was measured using the fluorescence dye-based microplate flux assay. PDKO platelets showed substantial inhibition of calcium mobilization in the presence of a physiological concentration of calcium (Fig. 7A). Moreover, calcium mobilization was also impaired when PDKO platelets were incubated under similar conditions without any supplemented calcium (Fig. 7B). Although we cannot eliminate the possibility that dematin regulates calcium homeostasis in platelets via modulation of plasma membrane-embedded calcium pumps, our data suggest that dematin is a key regulator of internal stores of calcium in platelets.

Activated platelets rely heavily on the release of calcium into the cytosol to regulate critical signaling cascades and overall platelet functions. Upon platelet activation, internal stores of calcium in the dense tubular network (DTS) are released into the cytosol, thus triggering external calcium influx via the Orai1 membrane calcium channel.[18,29,30] The store-operated calcium entry process and internal calcium release triggered by the generation of IP_3 from PLCγ2 enzymatic activity are key regulatory

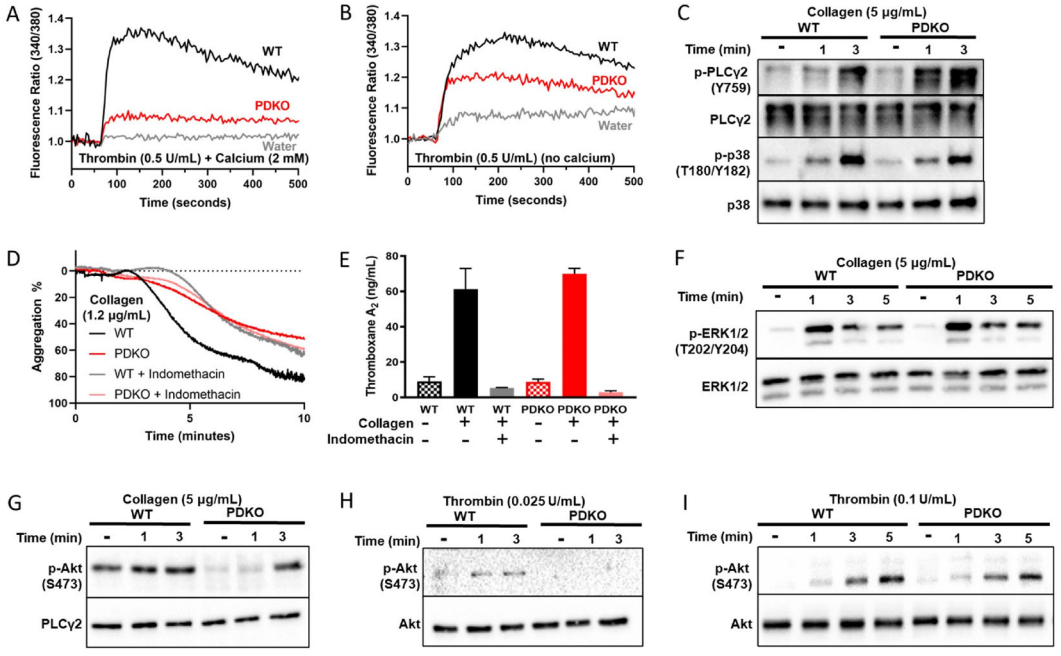

FIG 7 Mechanistic analysis of dematin's regulation of platelet activation pathways. (A) Calcium mobilization of WT and PDKO platelets after thrombin (0.5 U/mL) stimulation with supplemented calcium (2 mM). **(**B) Calcium mobilization of WT and PDKO platelets after thrombin (0.5 U/mL) stimulation without calcium. (C) Phosphorylation of WT and PDKO PLCγ2 (Y759) and p38 (T180/Y182) in resting conditions and after collagen (5 µg/mL) stimulation (1 and 3 min). (D) Collagen (1.2 µg/mL) stimulated aggregation of WT and PDKO platelets treated with or without indomethacin (10 µM). (E) Thromboxane A_2 measurements of WT and PDKO platelets resting, collagen stimulated (2 µg/mL), and collagen stimulated (2 µg/mL) with indomethacin (10 µM). WT: 8.49 ± 1.06; WT + collagen: 66.52 ± 10.50; WT + collagen + indomethacin: 5.18 ± 0.69; PDKO: 9.51 ± 0.94; PDKO + collagen: 69.96 ± 3.05; PDKO + collagen + indomethacin: 3.27 ± 0.10; PDKO versus WT *P* value 0.4155; PDKO + collagen versus WT + collagen *P* value 0.6997; PDKO + collagen + indomethacin versus WT + collagen + indomethacin *P* value 0.0595; all nonsignificant. **(**F) Phosphorylation of WT and PDKO ERK1/2 (T202/Y204) in resting conditions and after collagen (5 µg/mL) stimulation (1, 3, and 5 min). (G to I) Phosphorylation of WT and PDKO Akt (S473) using collagen (5 µg/mL) (G), and thrombin (0.025 U/mL) (H), and thrombin (0.1 U/mL) (I). Phosphorylation of platelets was measured under resting conditions and upon stimulation at 1-, 3-, and 5-min time points as indicated.

steps.[18,29] To investigate the role of dematin in this pathway, we measured the activation of PLCγ2 via phosphorylation at residue Y759 in response to platelet activation by collagen (5 μg/mL). During the initial phase of platelet activation, no statistically significant difference in the phosphorylation of PLCγ2 was observed between WT and PDKO platelets (Fig. 7C). This result suggests that PLCγ2 activity is unlikely to contribute to the striking calcium mobilization defect observed in PDKO platelets.

Platelet thromboxane A2 generation is independent of dematin. Another key regulator of platelet autocrine and paracrine signaling cascade is the release of thromboxane A_2 (TXA_2) modulating thromboxane receptors.[31–34] The generation of thromboxane is coordinated by the eicosanoid pathway wherein arachidonic acid processed by COX-1/2 into prostaglandin is subsequently converted into TXA_2.[35] To investigate a functional role of dematin in TXA_2 signaling, we measured platelet aggregation in response to collagen (1.2 μg/mL) in the presence and absence of indomethacin (10 μM), a reversible COX inhibitor. As expected, WT platelet aggregation was slower and incomplete within 10 min of collagen activation (Fig. 7D). In contrast, PDKO platelets, which are already deficient in platelet aggregation (Fig. 3), did not show any additional inhibitory effect upon indomethacin treatment (Fig. 7D). One possible cause for the lack of further aggregation defect could be that the complete loss of dematin in platelets limits TXA_2 production and therefore makes the indomethacin treatment insensitive to PDKO platelet aggregation. To test this possibility, we measured overall thromboxane B_2 (TXB_2) generation in WT and PDKO platelets. Due to the rapid nonenzymatic conversion of TXA_2, TXB_2 measurement is a more reliable readout of the overall thromboxane generation.[36] Platelets at the resting state and activated by collagen in the presence and absence of indomethacin (10 μM) pretreatment were evaluated for TXB_2 generation using a commercial ELISA kit (Cayman Chemical Company). Our data indicate that PDKO platelets showed similar TXB_2 levels under these conditions compared to WT platelets (Fig. 7E), indicating that the loss of dematin does not affect thromboxane levels in platelets.

Finally, to rule out the possibility that upstream enzymes in the thromboxane pathway may be affected in the PDKO platelets, we measured phosphorylation of p38 (T180/Y182) (Fig. 7C) and ERK1/2 (T202/Y204) (Fig. 7F) in response to collagen activation for up to 5 min. No effect of dematin deficiency was observed in p38 or ERK1/2 phosphorylation under these conditions (Fig. 7C and F). These results show that TXA_2 production is intact in PDKO platelets in response to collagen activation, and other mechanisms may regulate the dematin-mediated signaling in platelets.

Dematin is a novel mediator of early activation of Akt in platelets. Akt, also known as protein kinase B, is a potent signal transducer of multiple signaling functions in platelets. Upon stimulation by a variety of agonists, Akt activation occurs rapidly and mediates several downstream signaling cascades, including degranulation and PLCγ2 signaling, contributing to platelet activation.[37–39] Active Akt promotes outside-in signaling mediated by integrin αIIb/β3 upon post-ligand binding.[37] To investigate the status of Akt activation in PDKO platelets, we measured Akt phosphorylation (S473) at the early stage of platelet activation by multiple agonists. In response to collagen (5 μg/mL), PDKO platelets showed a near absence of Akt phosphorylation at basal levels and this inhibition persisted during the early phase of platelet activation (Fig. 7G). This Akt inhibition contrasts with WT platelets that undergo rapid phosphorylation of Akt after 1 min of agonist stimulation (Fig. 7G). At 3 min poststimulation of platelets by collagen, the PDKO platelets eventually restored Akt phosphorylation to WT levels (Fig. 7G).

To further confirm impaired Akt activation with other agonists, we measured platelet Akt phosphorylation (p-Akt) in response to thrombin. Upon stimulation by low concentrations of thrombin (0.025 U/mL), p-Akt was inhibited in PDKO platelets both at 1- and 3-min time points post-agonist stimulation (Fig. 7H). However, the p-Akt phosphorylation defect in PDKO platelets was rescued to WT levels at a higher concentration of thrombin (0.1 U/mL) (Fig. 7I). These results indicate that dematin is required

for the early activation of Akt in platelets. To our knowledge, this finding is the first demonstration that dematin regulates Akt signaling in platelets with broad implications in the regulation of cell shape change, aggregation, degranulation, and clot retraction pathways in platelets.

Dematin in platelets attenuates in vivo thrombosis. To determine the role of platelet dematin in thrombus formation in vivo, we employed a well-established laser-induced thrombosis model.[40,41] The mice lacking platelet dematin generated smaller thrombi as measured by both platelet accumulation (WT: 122×10^{15} RFU: KO: 3.72×10^{15} RFU; $P < 0.001$) and fibrin deposition (WT: 12.7×10^{15}; 1.32×10^{15} RFU; $P < 0.001$) than their litter-mate controls (Fig. 8). Thrombus formation in vivo was analyzed over 220 s, and representative pictures of the first 120 s are shown (Fig. 8A). In summary, these data suggest that mice lacking dematin in their platelets have a deficiency in clot formation.

DISCUSSION

Anucleate RBCs and platelets rely on their flexible spectrin-actin cytoskeletal network regulated by multiple adaptor proteins to withstand extreme shear stress during circulation. Actin is a major cytoskeletal component constituting ~15–20% of the total protein in platelets.[42] Therefore, there is considerable interest in understanding the regulation of actin reorganization in platelets, with functional implications in both shape change and downstream signaling pathways essential for hemostasis and thrombosis. Adducin and dematin are two major actin-binding proteins sharing structural and functional similarities between RBCs and platelets.[2,43] Here we report the first characterization of a mouse model with targeted deletion of full-length dematin in platelets.

Our first attempt to investigate dematin function in platelets started with the generation of a mouse model systemically lacking the headpiece domain of dematin (HPKO).[19] Initial hematological evaluation of the HPKO phenotype demonstrated mild anemia resulting from impaired RBC shape and membrane stability.[19] While not an ideal model system to study platelet physiology due to mild anemia, the characterization of HPKO platelets retaining the core domain of dematin revealed a functional role of dematin in calcium mobilization.[19] Subsequently, we generated a double knockout

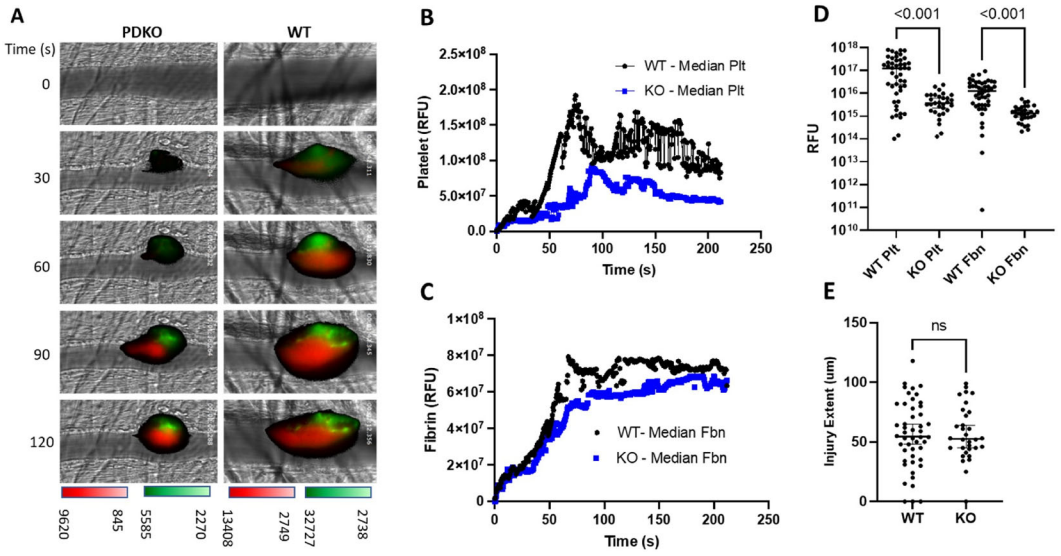

FIG 8 Thrombus formation is decreased in mice with platelets lacking dematin. Platelet accumulation and fibrin deposition following laser ablation of cremasteric arterioles were monitored in mice with a platelet/megakaryocyte-specific deficiency in dematin (PDKO) and in Cre-negative littermate control mice. (A) Representative images of thrombus formation taken at 30 second intervals. Platelets are represented in red and fibrin in green. Median curves of (B) platelet accumulation and (C) fibrin deposition in PDKO (blue squares) and WT controls (black circles) were plotted following laser ablation at time 0. (D) Areas under the curve from 0 to 200 s were calculated and plotted for all curves (PDKO: $n = 32$ thrombi; WT: $n = 48$ thrombi). (E) Injury size following laser ablation was measured to assess whether differences in platelet accumulation and fibrin deposition were due to differences in injury size.

mouse model (DAKO) systemically lacking both the headpiece domain of dematin and β-adducin.[13] Unlike the HPKO model, the DAKO mice showed severe erythrocyte membrane fragmentation and hemolysis.[13] While these studies were informative in revealing a redundant role of the dematin headpiece and β-adducin in erythrocytes, the DAKO mice were not suitable to study the physiological function of platelets in vivo due to severe hemolysis in vivo. Subsequent in vitro studies suggested an important role of the core domain of dematin in cell shape and cytoskeletal reorganization.[1,10,22] Therefore, we generated the FLKO mouse model with a systemic deletion of full-length dematin.[2] Consistent with the importance of the core domain of dematin, FLKO mice showed a precipitous loss of erythrocyte membrane stability and massive hemolytic anemia.[2] Again, the FLKO model was not suitable for functional studies on platelets. To circumvent these limitations, we have now developed a new mouse model carrying the platelet-specific deletion of full-length dematin (PDKO). The PDKO mice are viable with no evidence of anemia or impaired hemostasis (Fig. 1 and Fig. 2).

The localization of dematin to internal membranous structures in platelets suggested a potential mechanism of dematin function in the regulation of calcium.[19] It was proposed that dematin regulates the function of inositol 1,4,5-trisphosphate 3-kinase isoform B (*IP3KB*), which phosphorylates IP_3 to IP_4 thus regulating the release of internal calcium stores and calcium mobilization in platelets.[19] In addition, the upstream PLCγ2 cleaves PIP_2 into IP_3 and diacylglycerol (DAG) thus regulating signaling and calcium mobilization in platelets.[18,29,44] The development of the PDKO mouse model enabled us to evaluate the function of platelet dematin in various signaling pathways. Our results show that phosphorylation of PLCγ2, p38, and ERK1/2 appears to be normal in activated PDKO platelets (Fig. 7C and F). This observation suggests that the calcium mobilization defect observed in PDKO platelets is likely to be regulated by *IP3KB* located at the DTS, as indicated by our previous studies on HPKO model.[19] Since the calcium mobilization defect in PDKO platelets is observed both in the presence and absence of extracellular calcium (Fig. 7A and B), we cannot rule out the possibility that dematin may also regulate surface calcium channels and store-operated calcium entry regulators via biochemical interactions at the platelet plasma membrane.

Akt activation is a crucial early time point signaling nexus that mediates agonist-induced signaling cascades in platelets and potentially in other cells. Akt plays an important role in GPIb-IX-mediated early signals that lead to inside-out integrin activation in platelets.[38,39] Akt activation also promotes thromboxane synthesis and degranulation.[33] Degranulation occurs as a second wave of stimuli which is utilized to propagate platelet activation signals.[24,33,45] During platelet activation by U46619, a thromboxane analog, dense-granule release occurs in a distinct two-phase pattern[33] (Fig. 4D). In PDKO platelets, the first phase of U46619-induced activation is significantly diminished yet remains intact. Importantly, the second phase of ATP secretion is completely ablated in PDKO platelets (Fig. 4D). This second phase of dense-granule release in platelets is a PI3K/Akt-dependent process.[33] Given our observation that integrin activation is also inhibited in PDKO platelets (Fig. 5A and B), these data suggest that dematin may regulate the Akt-PI3K-Integrin signaling axis in platelets. This hypothesis is consistent with the inhibition of agonist-induced early Akt phosphorylation that recovered 3 min after stimulation of PDKO platelets (Fig. 7G to I).

Published Akt loss of function studies indicate that Akt is not required for platelet spreading on fibrinogen, which is governed by the outside-in signaling.[39] Our results show that PDKO platelets exhibit impaired spreading on fibrinogen-coated surfaces (Fig. 6A and B) as well as reduced clot retraction (Fig. 5C). These findings suggest that dematin may also play a functional role in outside-in integrin signaling in an Akt-independent manner. Our previous findings in HPKO platelets that retain the core domain of dematin did not show any measurable spreading defect on fibrinogen-coated surface.[19] Significant inhibition of PDKO platelet spreading on fibrinogen substrate (Fig. 6A and B) indicates that both core and headpiece domains of dematin are

required for regulating cell spreading in platelets. It is not known whether the headpiece domain of dematin or related family members is required for Akt activation, or whether the core domain alone is sufficient for early Akt activation in response to agonists. Furthermore, actin-rich lamellipodia are important cellular structures required for increasing platelet surface area during platelet activation and spreading.[46,47] SEM analysis showed a lack of lamellipodia in PDKO platelets (Fig. 6C), thus suggesting a unique role of dematin in establishing lamellipodia formation in platelets. The characterization of the PDKO model, as reported here, revealed dematin as a novel cytoskeletal regulator of cell shape, lamellipodia formation, and spreading, all outcomes of outside-in signaling in platelets. Together, our data suggest that dematin regulates outside-in signaling in an Akt-independent manner, concomitant with its essential role in platelet inside-out signaling.

An unexpected linkage between dematin, kindlin-3, and integrin has been previously identified vis-à-vis platelet activation and hemolytic anemia.[48,49] Kindlin-3 is expressed in erythrocytes, and kindlin-3 mutant mice show a dramatic reduction of dematin in the erythrocyte membranes.[48] Since both dematin and kindlin-3 are abundantly expressed in platelets, we decided to examine the impact of dematin deletion on kindlin-3 and integrin activation in PDKO mice (Fig. 5A and B). Western blot analysis showed no effect of dematin deletion on kindlin-3 expression in the resting and thrombin-activated platelets (Supplemental Fig. 3). Given that beta-adducin is also substantially reduced in kindlin-3 mutant erythrocytes,[48] there is a possibility that kindlin-3 deficient platelets may also show a reduction in beta-adducin.[50] Therefore, we cannot rule out the possibility that the generation of double knockouts mice lacking both dematin and adducin might produce synergistic effects on platelet integrin activation, aggregation, degranulation, shape change, clot retraction, and spreading as observed in the PDKO mice.

When dematin expression is lost in platelets, both the accumulation of platelets and the deposition of fibrin are attenuated at the site of a laser-induced injury in KO mice when compared to their littermate controls. Both the median accumulation curves (Fig. 8B and C) and areas under all curves (Fig. 8D) for both platelet and fibrin support this conclusion (Fig. 8A to D). The injury sizes, determined by assessing the longitudinal length of vessel wall damage caused by laser ablation, are similar in both the experimental and control conditions (Fig. 8E). These in vivo data are consistent with the platelet function studies demonstrating impaired platelet aggregation in platelets lacking dematin.

In summary, the selective and complete deletion of dematin in the PDKO model demonstrates a functional role of dematin in calcium mobilization and early phosphorylation of Akt post-agonist activation in platelets. Mechanistically, our findings support the integration of dematin into the model of platelet activation cascade regulated by calcium mobilization (Fig. 9). The absence of a bleeding phenotype in PDKO mice is relevant for the therapeutic targeting of dematin in future pharmacological and translational applications.

MATERIALS AND METHODS

Materials, antibodies, and reagents. The dematin monoclonal antibody used in this study was originally developed by the Chishti Lab in collaboration with BD Biosciences/Transduction Laboratories (#D77620). Multiple antibodies purchased from Cell Signaling Technologies (Danvers, MA, USA) are as follows: PLCγ2 (#3872); p-PLCγ2 (Y759) (#3874); Akt (#4691); p-Akt (S473) (#4058); p38 MAPK (#8690); p-p38 (T180/Y182) (#4511); p44/42 MAPK (ERK1/2) (#4695); p-p44/42 MAPK (ERK1/2) (T202/Y204) (#4377). Rat monoclonal GPIIb/IIIa antibody (also called αIIb/β3; JON/A active form) (Integrin alphaIIbbeta3 (GPIIb/IIIa, CD41/CD61)-PE) (#M023-2) was purchased from Emfret Analytics (Eibelstadt, Germany). Mouse CD62P (P-selectin) antibody (#553744) was purchased from BD Biosciences. AF594 Phalloidin peptide (#A12381) was purchased from Invitrogen. Thrombin (#60-519) was purchased from EMD Millipore. U46619 (#16450) was purchased from Cayman Chemical Company. Collagen (#NC9533954) was purchased from Chrono-Log. ADP (#A2754) was purchased from Sigma. Platelet agonist TRAP4 was generously provided by Dr. Lidija Covic (Tufts Medical Center, Boston, MA). Collagen-related peptide (CRP) was generously provided by Dr. Peter Newman (Milwaukee, WI). PGE1 (#BML-PG006) was purchased from Enzo Life Sciences. Indomethacin (#458030050) was purchased from Acros Organics.

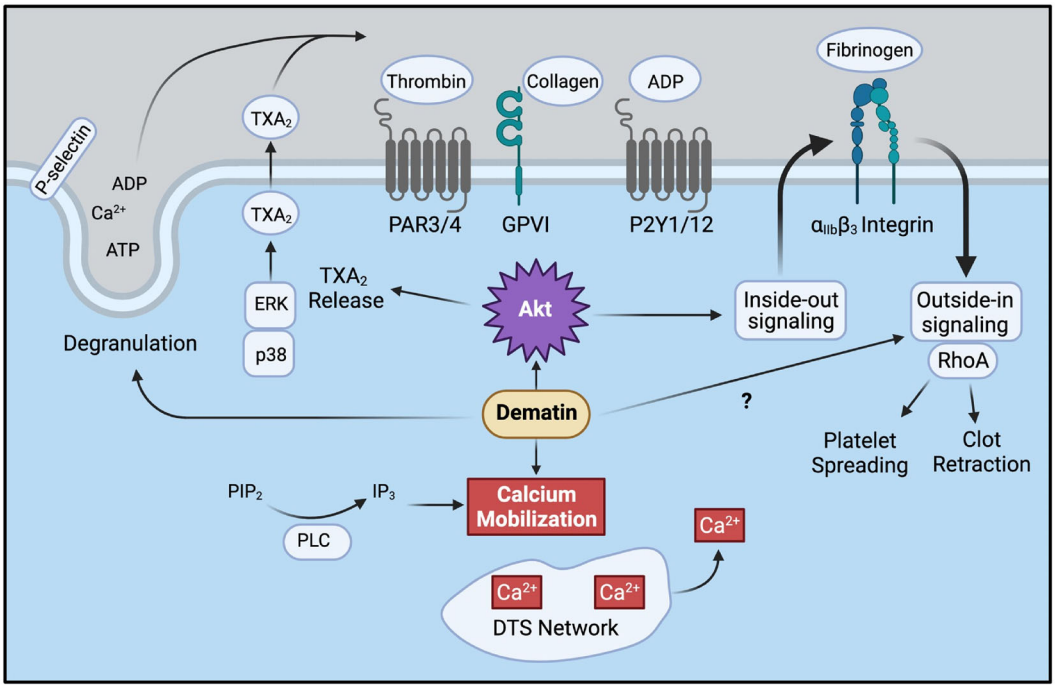

FIG 9 Primary platelet activation schematic incorporating the functional role of dematin. Dematin functions at a signaling nexus that (1) regulates Akt activation and subsequent signal transduction, (2) promotes calcium mobilization, and (3) mediates outside-in signaling. As a consequence, PDKO platelets display significantly impaired platelet activation phenotypes thus disrupting normal platelet functions.

FlexStation (Molecular Devices) was used for calcium measurements, and light transmission optical aggregometry was performed using the Chrono-Log Model 700 aggregometer.

Mice and genotyping. PDKO mice were derived from the FLKO model as previously described.[2] Mice homozygous for the mutated *DMTN* allele were crossed with FRT-expressing lines to generate *DMTN* floxed/floxed (*DMTN* f/f) alleles. PDKO mice were generated by crossing *DMTN* f/f mice with *DMTN* f/f mice heterozygous for Cre driven by the megakaryocyte-specific Pf4 promoter (Pf4-Cre). PDKO (*DMTN* f/f; Cre +/–) mice were produced from this cross at a Mendelian ratio of 1:1. Mice were genotyped using DNA digested from tail tip tissue and tested with two primer pairs. Cre expression was tested with Pf4-Cre forward primer: *CCA AGT CCT ACT GTT TCT CAC TC* and Pf4-Cre reverse primer: *TGC ACA GTC AGC AGG TT* resulting in a 400-base pair (bp) amplicon. *DMTN* f/f genotyping was performed using *DMTN* f/f forward primer: *GCC GGC TGA CTT AAG TGG GAT CC* and *DMTN* f/f reverse primer: *GTT TTC CAG GGT GAC AGC TGT TCA* resulting in a 351 bp amplicon. *DMTN* f/f; Pf4-Cre +/– mice were designated as "PDKO," while *DMTN* f/f; Pf4-Cre –/– mice were designated as "WT". Primers were designed and generated using Integrated DNA Technologies. Both WT and PDKO mice were apparently healthy upon visual inspection, with no weight or behavior disparities. No pathological mortality was observed. Differential dematin expression was further confirmed by Western blotting of purified washed platelets lysates and red blood cell membrane lysates and compared with a loading control antibody using standard techniques.

Platelet isolation. Blood was collected through venipuncture of the inferior vena cava using a 22-gauge needle and collected into 150 μL of acid citrate dextrose solution (trisodium citrate 2.5%, glucose 1.5%, citric acid 0.4%) supplemented with PGE1 (0.1 μg/mL). Blood samples were then mixed with an equivalent volume of modified Tyrode's buffer (137 mM NaCl, 10 mM HEPES, 12 mM $NaHCO_3$, 5 mM glucose, 2.5 mM KCl, 1.0 mM $MgCl_2$), incubated at 37 °C for 10 min, centrifuged at 200 *g* for 15 min in a swinging bucket centrifuge with no centrifuge braking to separate the platelet-rich plasma (PRP). PRP was harvested and incubated with 1.0 mM EDTA, rested at room temperature for 10 min, and spun at 600 *g* for 10 min to pellet the platelets. The platelet pellet was washed and resuspended with fresh Tyrode's buffer and then rested at 37 °C prior to quantification. Platelet samples were quantified based on OD600 measurements using the formula:

$$6.23/((2.016 - \text{OD600}) - 3.09) * \text{Dilution Factor} * 108 = \text{platelets/mL}$$

Samples were subsequently diluted and prepared for specific experiments.

CBC (complete blood count). Five hundred microliters of blood was harvested in EDTA tubes and submitted for comprehensive complete blood count analysis using IDEXX commercial service (product #61330). Results shown are representative of three separate samples submitted for CBC analysis.

Platelet aggregation and dense granule release. Freshly harvested platelets were diluted to a concentration of 3E8 platelets/mL. Using a Chrono-Log model 700 aggregometer set to 37 °C and stirrer spinning at 1200 rpm, platelet samples were supplemented with calcium (1.0 mM) immediately prior to agonist stimulation. Platelet aggregation was tested using various agonists indicated in the Results section. Platelets were pretreated with indomethacin (10 μM) 3 min prior to the agonist stimulation for the

designated experiments. Dense granule release was assessed using the Chrono-Lume reagent (Product #395) added and preincubated for 3 min before the agonist addition according to the manufacturer's specifications. Results shown are representative of at least three separate experiments.

Calcium mobilization. Washed platelets were diluted to a concentration of 7.5E8 platelets/mL and incubated with FURA 2AM/LR (15 μM, Millipore product #344911) for 45 min at room temperature in the dark. Platelets were then washed and resuspended at a minimum concentration of 1E8 platelets/mL. Calcium measurements were made with a FlexStation plate reader (Molecular Devices) at 340 nm and 380 nm excitation and 510 nm emission. Wavelength ratios (340/380) were plotted after baseline normalization. Results shown are representative of three separate experiments.

Clot retraction. PRP was isolated from whole mouse blood and platelet volume was equilibrated using Tyrode's buffer in a tube with an end-sealed glass pipette. Three hundred and fifty microliters of platelet suspension was supplemented with a small volume of packed RBCs to enhance the contrast of the clot. Platelets were treated with calcium (2.0 mM) and then stimulated with thrombin (1.0 U/mL and 0.5 U/mL). Photographs were taken at the indicated time intervals over 24 h. Results shown are representative of three separate experiments.

Thromboxane measurements. Mouse platelet samples were diluted to 1E8 platelets/mL and transferred to a Chrono-Log model 700 aggregometer at 37 °C and stirred at 1000 rpm. Indomethacin (10 μM) treated samples were incubated for 10 min prior to activation. Agonists were added to samples and incubated for 10 min. Samples were transferred to microcentrifuge tubes and platelets were pelleted by centrifugation at 600 g for 10 min. Supernatants were extracted and diluted for preparation of the thromboxane B_2 ELISA (Cayman Chemical Company, #501020) according to the manufacturer's instructions. Results shown are representative of three separate experiments.

Platelet protein lysates and western blotting. Washed platelets were adjusted to 4E8 platelets/mL, and platelet suspension was incubated in a Chrono-Log model 700 aggregometer at 37 °C and spinning at 1200 rpm. Platelets were supplemented with 1.0 mM calcium and stimulated by the indicated agonists or left resting. At corresponding time points, platelet stimulation was halted by cell lysis through the addition of 5X reducing sample buffer (0.5 M sucrose, 15% SDS, 312.5 mM Tris-HCl, pH 6.9, 10 mM EDTA). SDS-PAGE and Western blotting were performed using standard techniques. Anti-kindlin-3 (D817V) rabbit mAb (Cell Signaling Technology) and anti-kindlin-3 (2F3) mouse mAb (Dr. Edward Plow, Cleveland Clinic) were used to detect kindlin-3 in PDKO platelets. Results shown are representative of at least three separate experiments.

Tail bleeding hemostasis assay. Mouse tail bleeding assays were performed as described before[51] by cutting approximately 2 mm of mouse tail tip tissue using surgical scissors. The tail wound was submerged in 37 °C saline and bleeding time was recorded. Statistical medians were determined using GraphPad Prism software.

Platelet spreading assay. Coverslips (12 mm diameter, #1.5) were coated with human fibrinogen (100 μg/mL) (Sigma-Aldrich #F3879) in 0.1 M $NaHCO_3$ at 4 °C overnight. Coverslips were then washed with $NaHCO_3$ and blocked with 5% BSA in $NaHCO_3$ for 90 min. Mouse platelets at 3.5E7 platelets/mL were incubated on the coverslips for times indicated in the experiments at 37 °C. The supernatant was removed, and the coverslips were washed with PBS and fixed in 4% paraformaldehyde for 15 min at room temperature. After two PBS washes, the samples were incubated with permeabilization buffer (100 mM, Tris-HCl pH 7.4, 10 mM EGTA, 154 mM NaCl, 5 mM $MgCl_2$, 0.1% Triton X-100), with protease inhibitor cocktail tablets (Roche #1183617000) for 10 min at 4 °C. After washing with PBS, samples were blocked with 5% BSA in PBS for 15 min. Phalloidin AF594 (1.65 μM, Thermo Fisher A12381) in 5% BSA buffer was incubated with the samples for 30 min at 4 °C in the dark followed by PBS washing and drying of the coverslips. Coverslips were mounted using ProLong Antifade mountant (Thermo Fisher #P36962) and rested overnight at 4 °C in the dark before imaging. Imaging was performed using a Nikon TE2000-E microscope and Nikon pco.edge camera. Nikon Elements imaging software was used for the measurement of cell area. Statistical analysis was performed using GraphPad Prism software using either Student's *t-tests* or two-way ANOVA. The results shown are representative of at least five separate experiments.

Scanning electron microscopy of platelet spreading. Coverslips (12 mm diameter, #1.5) were coated with human fibrinogen (100 μg/mL) (Sigma-Aldrich #F3879) in 0.1 M $NaHCO_3$ and incubated at 4 °C overnight. The coverslips were then washed with $NaHCO_3$ and incubated with 5% BSA in $NaHCO_3$ for 90 min. Mouse platelets at a concentration of 3E7 platelets/mL were incubated on the coverslips for times indicated in the experiments. Samples were incubated in 2% paraformaldehyde/2% glutaraldehyde fixative in sodium cacodylate buffer (100 mM) at ambient temperature. After fixation, samples were incubated in 1% Osmium tetroxide in 0.1 M sodium cacodylate buffer, pH 7.4, for 1–2 h. Samples were dehydrated by stepwise immersion in an ethanol gradient and dried in a critical point dryer. Samples were then sputter-coated in Palladium and viewed in a Hitachi S-4700 FESEM at the Harvard Medical School Electron Microscopy facility (Boston, MA, USA). Results shown are representative of three separate experiments.

Flow cytometry analysis of α-granule release and integrin activation. Freshly isolated platelets were diluted to 4E7 platelets/mL and supplemented with 1.0 mM calcium. Platelet samples (25 μL) were incubated with agonists (5 μL, 7X relative dilution) and fluorescent antibodies (5 μL, 7X relative dilution) for 15 min. PBS (400 μL) was added to dilute the sample and terminate the reaction, and samples were analyzed in an LSRII flow cytometer (BD Biosciences) within 30 min. FACSDiva software (BD Biosciences) was used for the quantitation of mean fluorescence values. FlowJo software was used for graphical representations of data. Flow cytometry was performed based on established protocols from Emfret Analytics (Eibelstadt, Germany; emfret.com). The results shown are representative of at least five separate experiments.

Measurement of rho-GTPase activity in mouse platelets. Washed platelets were adjusted to 3E8 platelets/mL and activated for 1 min with thrombin either with 0.3 U/mL or 0.5 U/mL. Platelet samples were lysed and prepared according to the manufacturer's protocol for the RhoA ELISA (Cytoskeleton Inc., #BK124-S). The activated RhoA readout was measured by the colorimetric emission at 490 nm in a plate reader. The results shown are representative of three separate experiments with three replicates per condition.

Induction of in vivo thrombosis. Laser-induced thrombosis in mice was performed as previously described.[40] Briefly, mouse platelets were labeled using a platelet specific β3 integrin antibody conjugated to DyLight 649 (Emfret Analytics, Eibelstadt Germany). The progression of fibrin formation was detected using a fibrin-specific antibody (clone 59D8, labeled with DyLight 488). Laser-induced injuries triggered platelet accumulation and fibrin deposition at the site of injury, and fluorescent intensities over time were recorded. Three mice were analyzed for each condition with 10–15 observations per mouse.

Statistics. Statistical significance for all methods with the exception of laser-induced thrombosis, was determined using a Student's unpaired *t-test* where $P < 0.05$ and $P < 0.01$. Laser-induced thrombosis significance was determined using the Mann–Whitney test on area under the curve median fluorescent intensity values of either platelet accumulation or fibrin deposition over time.

SUPPLEMENTAL MATERIAL

Supplemental data for this article can be accessed online at https://doi.org/10.1080/10985549.2023.2210033.

ACKNOWLEDGEMENTS

We thank Dr. Peter Newman of Blood Research Institute, Milwaukee, Wisconsin, for generously sharing the collagen-related peptide (CRP) for platelet activation studies. We also thank Dr. Lidija Covic of Tufts Medical Center, Boston, MA, for sharing the TRAP4 agonist for initial studies of platelet activation. Dr. Covic's technical guidance for the calcium mobilization experiments was invaluable. Anti-kindlin-3 antibodies were kindly provided by Dr. Edward Plow (Cleveland Clinic) and Dr. Stephen C. Bunnell (Tufts University). We thank Stephen Kwok (Tufts Core Flow Cytometry Facility) for invaluable guidance with the flow cytometry measurements. Finally, we thank Donna-Marie Mironchuk for her many contributions to the administrative organization of the project, proofreading, and improvements of figures. Figure 9 was created with BioRender.com.

AUTHORS' CONTRIBUTIONS

Contributions: DF, TH, and AC conceived and designed the study. TH generated the PDKO mice. DF performed all the major experiments reported in this study. The in vivo thrombosis experiments (Fig. 8) were performed by GM-S using the resources and advice from RF. RF provided critical feedback during the course of this study. YD played a pivotal role in the characterization and genotyping of PDKO mice and data reported in Fig. 1 to Fig. 3 and Fig. 7 as well as kindlin-3 expression analysis (Supplemental Fig. 3). DF wrote the first draft of the manuscript. AC edited the manuscript and guided the project from its inception to completion. All authors edited various versions of the manuscript and approved the final manuscript.

FUNDING

This work was supported in part by grants from the National Heart, Lung, and Blood Institute (NHLBI) [RO1-HL060961 (AC), R01-HL095050 (AC), R35HL135775 (RF)], Tufts Collaborates Seed Grant Program (AC), American Heart Association Grant-in-Aid [15GRNT25710346 (AC)], and American Heart Association Predoctoral Fellowship to Daniel Fritz [20PRE35210897; 2020-2021].

ORCID

Athar H. Chishti http://orcid.org/0000-0003-0335-1861

DATA AVAILABILITY STATEMENT

The data that support the findings of this study are available from the corresponding author, (AC), upon reasonable request.

REFERENCES

1. Khanna R, Chang SH, Andrabi S, Azam M, Kim A, Rivera A, Brugnara C, Low PS, Liu SC, Chishti AH. Headpiece domain of dematin is required for the stability of the erythrocyte membrane. Proc Natl Acad Sci U S A. 2002; 99:6637–6642. doi:10.1073/pnas.052155999.
2. Lu Y, Hanada T, Fujiwara Y, Nwankwo JO, Wieschhaus AJ, Hartwig J, Huang S, Han J, Chishti AH. Gene disruption of dematin causes precipitous loss of erythrocyte membrane stability and severe hemolytic anemia. Blood. 2016;128:93–103. doi:10.1182/blood-2016-01-692251.
3. Azim AC, Knoll JH, Beggs AH, Chishti AH. Isoform cloning, actin binding, and chromosomal localization of human erythroid dematin, a member of the villin superfamily. J Biol Chem. 1995;270:17407–17413. doi:10.1074/jbc.270.29.17407.
4. Rana AP, Ruff P, Maalouf GJ, Speicher DW, Chishti AH. Cloning of human erythroid dematin reveals another member of the villin family. Proc Natl Acad Sci U S A. 1993;90:6651–6655. doi:10.1073/pnas.90.14.6651.
5. Vardar D, Chishti AH, Frank BS, Luna EJ, Noegel AA, Oh SW, Schleicher M, McKnight CJ. Villin-type headpiece domains show a wide range of F-actin-binding affinities [Research Support, Non-U.S. Gov't Research Support, U.S. Gov't, P.H.S.]. Cell Motil Cytoskeleton. 2002;52:9–21. doi:10.1002/cm.10027.
6. Roof DJ, Hayes A, Adamian M, Chishti AH, Li T. Molecular characterization of abLIM, a novel actin-binding and double zinc finger protein. J Cell Biol. 1997;138:575–588. doi:10.1083/jcb.138.3.575.
7. Husain-Chishti A, Faquin W, Wu CC, Branton D. Purification of erythrocyte dematin (protein 4.9) reveals an endogenous protein kinase that modulates actin-bundling activity. J Biol Chem. 1989;264:8985–8991. doi:10.1016/S0021-9258(18)81891-9.
8. Husain-Chishti A, Levin A, Branton D. Abolition of actin-bundling by phosphorylation of human erythrocyte protein 4.9. Nature. 1988;334:718–721. doi:10.1038/334718a0.
9. Vugmeyster L, McKnight CJ. Phosphorylation-induced changes in backbone dynamics of the dematin headpiece C-terminal domain. J Biomol NMR. 2009;43:39–50. doi:10.1007/s10858-008-9289-4.
10. Chen L, Brown JW, Mok YF, Hatters DM, McKnight CJ. The allosteric mechanism induced by protein kinase A (PKA) phosphorylation of dematin (band 4.9). J Biol Chem. 2013;288:8313–8320. doi:10.1074/jbc.M112.438861.
11. Kim AC, Azim AC, Chishti AH. Alternative splicing and structure of the human erythroid dematin gene. Biochim Biophys Acta. 1998;1398:382–386. doi:10.1016/s0167-4781(98)00078-5.
12. Rubio-Moscardo F, Blesa D, Mestre C, Siebert R, Balasas T, Benito A, Rosenwald A, Climent J, Martinez JI, Schilhabel M, et al. Characterization of 8p21.3 chromosomal deletions in B-cell lymphoma: TRAIL-R1 and TRAIL-R2 as candidate dosage-dependent tumor suppressor genes. Blood. 2005;106:3214–3222. doi:10.1182/blood-2005-05-2013.
13. Chen H, Khan AA, Liu F, Gilligan DM, Peters LL, Messick J, Haschek-Hock WM, Li X, Ostafin AE, Chishti AH. Combined deletion of mouse dematin-headpiece and beta-adducin exerts a novel effect on the spectrin-actin junctions leading to erythrocyte fragility and hemolytic anemia. J Biol Chem. 2007;282:4124–4135. doi:10.1074/jbc.M610231200.
14. Patel-Hett S, Wang H, Begonja AJ, Thon JN, Alden EC, Wandersee NJ, An X, Mohandas N, Hartwig JH, Italiano JE. Jr. The spectrin-based membrane skeleton stabilizes mouse megakaryocyte membrane systems and is essential for proplatelet and platelet formation. Blood. 2011;118:1641–1652. doi:10.1182/blood-2011-01-330688.
15. Durrant TN, van den Bosch MT, Hers I. Integrin alpha(IIb)beta(3) outside-in signaling. Blood. 2017;130:1607–1619. doi:10.1182/blood-2017-03-773614.
16. Hsu-Lin S, Berman CL, Furie BC, August D, Furie B. A platelet membrane protein expressed during platelet activation and secretion. Studies using a monoclonal antibody specific for thrombin-activated platelets. J Biol Chem. 1984;259:9121–9126. doi:10.1016/S0021-9258(17)47274-7.
17. Shattil SJ, Newman PJ. Integrins: dynamic scaffolds for adhesion and signaling in platelets. Blood. 2004;104:1606–1615. doi:10.1182/blood-2004-04-1257.
18. Varga-Szabo D, Braun A, Nieswandt B. Calcium signaling in platelets. J Thromb Haemost. 2009;7:1057–1066. doi:10.1111/j.1538-7836.2009.03455.x.
19. Wieschhaus AJ, Le Breton GC, Chishti AH. Headpiece domain of dematin regulates calcium mobilization and signaling in platelets. J Biol Chem. 2012;287:41218–41231. doi:10.1074/jbc.M112.364679.
20. Faquin WC, Husain A, Hung J, Branton D. An immunoreactive form of erythrocyte protein 4.9 is present in non-erythroid cells. Eur J Cell Biol. 1988;46:168–175.
21. Cines DB, Lebedeva T, Nagaswami C, Hayes V, Massefski W, Litvinov RI, Rauova L, Lowery TJ, Weisel JW. Clot contraction: compression of erythrocytes into tightly packed polyhedra and redistribution of platelets and fibrin. Blood. 2014;123:1596–1603. doi:10.1182/blood-2013-08-523860.
22. Mohseni M, Chishti AH. The headpiece domain of dematin regulates cell shape, motility, and wound healing by modulating RhoA activation. Mol Cell Biol. 2008;28:4712–4718. doi:10.1128/MCB.00237-08.
23. Golebiewska EM, Poole AW. Platelet secretion: From haemostasis to wound healing and beyond. Blood Rev. 2015;29:153–162. doi:10.1016/j.blre.2014.10.003.
24. Jonnalagadda D, Izu LT, Whiteheart SW. Platelet secretion is kinetically heterogeneous in an agonist-responsive manner. Blood. 2012;120:5209–5216. doi:10.1182/blood-2012-07-445080.
25. Poll C, Westwick J. Phorbol esters modulate thrombin-operated calcium mobilisation and dense granule release in human platelets. Biochim Biophys Acta. 1986;886:434–440. doi:10.1016/0167-4889(86)90179-5.
26. Shattil SJ. Integrins and Src: dynamic duo of adhesion signaling. Trends Cell Biol. 2005;15:399–403. doi:10.1016/j.tcb.2005.06.005.
27. Pleines I, Hagedorn I, Gupta S, May F, Chakarova L, van Hengel J, Offermanns S, Krohne G, Kleinschnitz C, Brakebusch C, et al. Megakaryocyte-specific RhoA deficiency causes macrothrombocytopenia and defective platelet activation in hemostasis and thrombosis. Blood. 2012;119:1054–1063. doi:10.1182/blood-2011-08-372193.
28. Vogt AM, Barragan A, Chen Q, Kironde F, Spillmann D, Wahlgren M. Heparan sulfate on endothelial cells mediates the binding of Plasmodium falciparum-infected erythrocytes via the DBL1alpha domain of PfEMP1. Blood. 2003;101:2405–2411. doi:10.1182/blood-2002-07-2016.
29. Berridge MJ, Bootman MD, Roderick HL. Calcium signalling: dynamics, homeostasis and remodelling. Nat Rev Mol Cell Biol. 2003;4:517–529. doi:10.1038/nrm1155.
30. Jardin I, Albarran L, Bermejo N, Salido GM, Rosado JA. Homers regulate calcium entry and aggregation in human platelets: a role for Homers in the association between STIM1 and Orai1. Biochem J. 2012;445:29–38. doi:10.1042/BJ20120471.
31. Djellas Y, Manganello JM, Antonakis K, Le Breton GC. Identification of Galpha13 as one of the G-proteins that couple to human platelet thromboxane A2 receptors. J Biol Chem. 1999;274:14325–14330. doi:10.1074/jbc.274.20.14325.
32. Knezevic I, Borg C, Le Breton GC. Identification of Gq as one of the G-proteins which copurify with human platelet thromboxane A2/prostaglandin H2 receptors. J Biol Chem. 1993;268:26011–26017. doi:10.1016/S0021-9258(19)74486-X.
33. Li Z, Zhang G, Le Breton GC, Gao X, Malik AB, Du X. Two waves of platelet secretion induced by thromboxane A2 receptor and a critical role for phosphoinositide 3-kinases. J Biol Chem. 2003;278:30725–30731. doi:10.1074/jbc.M301838200.
34. Manne BK, Munzer P, Badolia R, Walker-Allgaier B, Campbell RA, Middleton E, Weyrich AS, Kunapuli SP, Borst O, Rondina MT. PDK1 governs thromboxane generation and thrombosis in platelets by regulating activation of Raf1 in the MAPK pathway. J Thromb Haemost. 2018;16:1211–1225. doi:10.1111/jth.14005.
35. Smith WL, DeWitt DL, Garavito RM. Cyclooxygenases: structural, cellular, and molecular biology. Annu Rev Biochem. 2000;69:145–182. doi:10.1146/annurev.biochem.69.1.145.
36. Patrono C, Ciabattoni G, Pugliese F, Pierucci A, Blair IA, FitzGerald GA. Estimated rate of thromboxane secretion into the circulation of normal humans. J Clin Invest. 1986;77:590–594. doi:10.1172/JCI112341.
37. O'Brien KA, Gartner TK, Hay N, Du X. ADP-stimulated activation of Akt during integrin outside-in signaling promotes platelet spreading by inhibiting glycogen synthase kinase-3beta. Arterioscler Thromb Vasc Biol. 2012;32:2232–2240. doi:10.1161/ATVBAHA.112.254680.
38. Woulfe DS. Akt signaling in platelets and thrombosis. Expert Rev Hematol. 2010;3:81–91. doi:10.1586/ehm.09.75.
39. Yin H, Stojanovic A, Hay N, Du X. The role of Akt in the signaling pathway of the glycoprotein Ib-IX induced platelet activation. Blood. 2008;111:658–665. doi:10.1182/blood-2007-04-085514.
40. Falati S, Gross P, Merrill-Skoloff G, Furie BC, Furie B. Real-time in vivo imaging of platelets, tissue factor and fibrin during arterial thrombus formation in the mouse . Nat Med. 2002;8:1175–1181. doi:10.1038/nm782.

41. Furie B, Furie BC. Thrombus formation in vivo. J Clin Invest. 2005;115: 3355–3362. doi:10.1172/JCI26987.
42. Bearer EL, Prakash JM, Li Z. Actin dynamics in platelets. Int Rev Cytol. 2002;217:137–182. doi:10.1016/s0074-7696(02)17014-8.
43. Barkalow KL, Italiano JE, Jr., Chou DE, Matsuoka Y, Bennett V, Hartwig JH. Alpha-adducin dissociates from F-actin and spectrin during platelet activation. J Cell Biol. 2003;161:557–570. doi:10.1083/jcb.200211122.
44. Wonerow P, Pearce AC, Vaux DJ, Watson SP. A critical role for phospholipase Cgamma2 in alphaIIbbeta3-mediated platelet spreading. J Biol Chem. 2003;278:37520–37529. doi:10.1074/jbc.M305077200.
45. Li Z, Delaney MK, O'Brien KA, Du X. Signaling during platelet adhesion and activation. Arterioscler Thromb Vasc Biol. 2010;30:2341–2349. doi:10.1161/ATVBAHA.110.207522.
46. Flevaris P, Stojanovic A, Gong H, Chishti A, Welch E, Du X. A molecular switch that controls cell spreading and retraction. J Cell Biol. 2007;179: 553–565. doi:10.1083/jcb.200703185.
47. Hall A. Rho GTPases and the control of cell behaviour. Biochem Soc Trans. 2005;33:891–895. doi:10.1042/BST20050891.
48. Kruger M, Moser M, Ussar S, Thievessen I, Luber CA, Forner F, Schmidt S, Zanivan S, Fassler R, Mann M. SILAC mouse for quantitative proteomics uncovers kindlin-3 as an essential factor for red blood cell function. Cell. 2008;134:353–364. doi:10.1016/j.cell.2008.05.033.
49. Moser M, Nieswandt B, Ussar S, Pozgajova M, Fassler R. Kindlin-3 is essential for integrin activation and platelet aggregation. Nat Med. 2008;14: 325–330. doi:10.1038/nm1722.
50. Hartwig JH, DeSisto M. The cytoskeleton of the resting human blood platelet: structure of the membrane skeleton and its attachment to actin filaments. J Cell Biol. 1991;112:407–425. doi:10.1083/jcb.112.3.407.
51. Novak EK, Sweet HO, Prochazka M, Parentis M, Soble R, Reddington M, Cairo A, Swank RT. Cocoa: a new mouse model for platelet storage pool deficiency. Br J Haematol. 1988;69:371–378. doi:10.1111/j.1365-2141.1988.tb02376.x.